

## Chapter 2

# Thermodynamics of Crystal-Melt Phase Change

### 2.1 Enthalpy: Heat and Work Exchanges in Solid-Liquid Transformations

The enthalpy, or heat content, provides a useful thermodynamic state function [1] when dealing with the energetic changes encountered in many types of solidification and melting processes, especially when they are carried out under constant pressure (isobaric) conditions. The enthalpy,  $H(S, P, N)$ , is an extensive thermodynamic property of a phase, derived as the Legendre transform [2] of the internal energy,  $U(S, V, N)$ , already used in Chapter 1.<sup>1</sup> In the particular case of the enthalpy, however, pressure,  $P$ , replaces volume,  $V$ , as one of the independent variables, and  $S$  and  $N$  remain the system's molar entropy and mass, respectively. In this instance, adding the pressure-volume product,  $PV$ , to the internal energy,  $U$ , provides the Legendre transform of the internal energy called enthalpy, or heat content,  $H(S, P, N)$ . Consequently, the molar enthalpies of a pure solid phase,  $s$ , and its conjugate melt phase,  $\ell$ , are found as,

$$H_i = U_i + PV_i \quad (i = s, \ell). \quad (2.1)$$

The enthalpy provides a direct measure of the energy increase of a system as heat is added at constant pressure. Consequently, the enthalpy is often the best choice for a thermodynamic state variable when tracking energy changes during solidification processes involving isobaric heat transfer. The total differential of the function defined in Eq. (2.1) is

$$dH_i = dU_i + PdV_i + V_i dP, \quad (2.2)$$

where we note that the last term on the RHS of Eq. (2.2) vanishes for changes occurring at constant pressure, where  $dP = 0$ .

---

<sup>1</sup> See Appendix A for details to derive any of the thermodynamic potentials from the internal energy function.

Now, the infinitesimal change in internal energy,  $dU_i$ , for a single-phase system of fixed mass receiving or releasing heat at constant pressure consists of differential changes in the heat,  $Q$ , and work,  $W$ . As is expressed by the 1st law of thermodynamics,

$$dU = \hat{d}Q + \hat{d}W. \quad (2.3)$$

The symbol,  $\hat{d}$ , in Eq. (2.3) is used to denote an ‘inexact’, or path-dependent, differential operator.<sup>2</sup> If the work involved with a melting or solidification process is restricted to ordinary mechanical pressure-volume work, then the RHS of Eq. (2.3) may be written as

$$dU_i = TdS_i - PdV_i, \quad (2.4)$$

where the differential of the heat added or subtracted via ‘reversible’ heat transfer from the system’s surroundings at temperature,  $T$ , is given by Clausius’s entropy formula,

$$\hat{d}Q_{rev} = TdS_i \quad (i = s, \ell). \quad (2.5)$$

Here  $dS_i$  is the differential change of the entropy of phase  $i$ . The molar, or gram-atomic entropy of a phase,  $S_i(U_i, V_i)$ , as indicated, is a thermodynamic state function of the extensive variables for an Avogadro’s number of particles ( $\approx 6.0221 \times 10^{23}$ ), i.e., for a unit molar, or gram-atomic mass. Reversible heat transfer, wherein heat energy is transferred to or from the surroundings of a thermodynamic system under the action of a *negligibly small* thermal gradient, provides the classical method for calculating entropy changes by integration of Eq. (2.5). The more general statement for a real irreversible processes is the so-called Clausius inequality,

$$\Delta S_{tot} \geq 0. \quad (2.6)$$

Equation (2.6) constitutes one of thermodynamic’s most important theoretical constructs, defining the *total* change of the entropy as always unidirectional, i.e., becoming more positive. This is a form of the 2nd law of thermodynamics, the deeper implication of which is that real processes spontaneously run in one direction, and in one direction only. Unless the transfer of heat energy to or from a phase, and all the attendant internal changes proceed infinitesimally slowly, the total entropy change (including unavoidable frictional or viscous processes) will be positive. All real processes, such as melting and solidification, of course, are always to some extent

---

<sup>2</sup> Its purpose here is to remind the reader that the amount of heat and work added to a system both depend on the particular path, or process, taken between arbitrary starting and ending thermodynamic states. Heat and work are *not* state functions, but their combined changes equal that of the internal energy, which is a state function.

‘irreversible’, and invariably involve the presence of entropy-increasing dissipation. All real processes, without exception, require that the *total* entropy change of the system and its environment increases, i.e.,  $\Delta S \geq 0$ . For an excellent introductory discussion on thermodynamic reversibility and irreversibility and the second law see [3].

Substituting Eq. (2.4) into Eq. (2.2) yields the well-known differential expression connecting the entropy change at constant pressure,  $dS_i$  of a phase ( $i = s, \ell$ ) with its corresponding change in enthalpy,  $dH_i$ .

$$dH_i = TdS_i. \quad (P = \text{const.}) \quad (2.7)$$

At constant pressure, which is the environment often encountered in ordinary solidification and melting processes, one may integrate Eq. (2.7) between a pair of states *A* and *B* and obtain

$$\Delta H_i = \int_A^B TdS_i = \Delta Q. \quad (P = \text{const.}) \quad (2.8)$$

Equation (2.8) shows formally that enthalpy changes are exactly equal to the *reversible* heat exchanges between a phase and its environment, the latter chosen in this instance to maintain the system’s pressure constant. That is, the heat energy,  $\Delta Q$ , transferred reversibly under steady pressure, by heating or cooling a phase, or by transforming it from solid to liquid, or vice versa, is equal to the changes in the system’s enthalpy function.

Equation (2.8) also demonstrates an extremely useful property of the enthalpy function that allows one to sketch an enthalpy-temperature phase diagram for a pure substance, held at fixed pressure, exhibiting an equilibrium melting (or freezing) point,  $T_{eq}$ .

The enthalpy-temperature phase diagram, Fig. 2.1, shows that the equilibrium liquid and solid occupy distinct, non-overlapping regions within the  $H$ - $T$  plane, with  $P$  fixed. Specifically, either solid or liquid exists as the preferred phase anywhere along their individual existence lines, each located, respectively, below and above the thermodynamic transition point,  $T_{eq}$ . A discontinuity in the enthalpy function always occurs at  $T_{eq}$  between the two-phase existence lines. This enthalpy ‘jump’ locates the unique combination of pressure and temperature at which the substance can exist in either, or both, phase states, depending on the system’s total heat content, or enthalpy. The enthalpy jump acts as a tie-line passing through a mixed-state, where both phases can coexist in equilibrium, in proportions that depend on the system’s overall enthalpy level. The enthalpy of the mixed (solid plus liquid) state may therefore vary between  $H_s(T_{eq})$ , for 100% solid, up to  $H_\ell(T_{eq})$  for 100% liquid. Enthalpy values intermediate between  $H_s$  and  $H_\ell$  correspond to a mole of solid-plus-liquid, with the lever rule and rule of mixtures controlling the exact proportions of these phases at equilibrium. More importantly, a two-phase mixture produced by solidification (even of a pure substance) represents, in actuality, a *solidification microstructure*. Solid-liquid microstructures consist of these

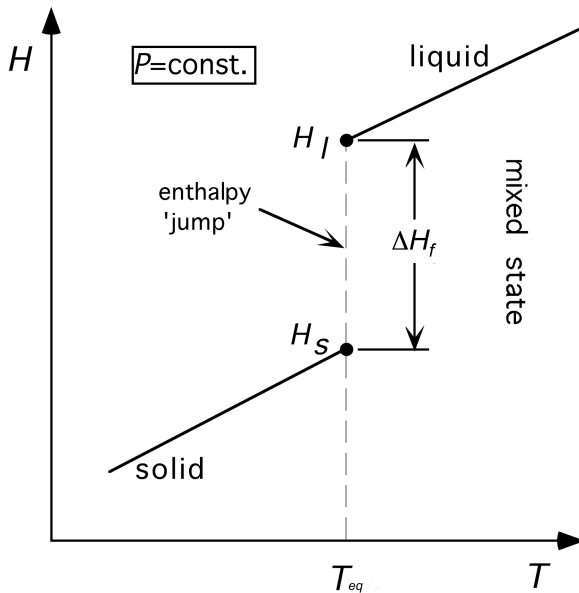


**Fig. 2.1** Enthalpy-temperature phase diagram for a pure substance. The enthalpy jump,  $\Delta H_f$ , represents the difference in heat content per unit mass of liquid and solid at their equilibrium melting-freezing point,  $T_{eq}$ . The difference in heat content is proportional to the entropy difference between the well-ordered crystalline solid state having low entropy, and the much less orderly (amorphous) liquid state having high entropy

phases in intimate, temporal contact, on length scales established by kinetic and other extrinsic factors, all of which reside beyond the scope of classical thermodynamics. The reader will find the kinetics of microstructure formation caused by different solidification processes discussed in considerable detail in later chapters, after various preliminary concepts are developed, including thermodynamics, heat and mass transfer, interfacial phenomena, and morphological stability.

In the case of isobaric equilibrium melting, the enthalpy-temperature phase diagram also shows that the jump in the heat content of the coexisting phases at  $T_{eq}$  defines an important property of the phase transformation itself, namely, the gram-atomic, or molar latent heat of fusion,  $\Delta H_f$ . This enthalpy difference between crystal and melt, per unit molar mass of substance, is indicated in Fig. 2.1 as

$$\Delta H_f = H_\ell(T_{eq}) - H_s(T_{eq}) \geq 0. \quad (2.9)$$

The inequality indicated on the RHS of Eq. (2.9), consistent with Fig. 2.1, states that upon melting, the jump in heat content is positive. Indeed, common experience shows that most materials do melt upon heating.<sup>3</sup> There are, however, a few

<sup>3</sup> The less common occurrence of melting upon cooling occurs in the case of metatectic systems [4].

exceptions to this rule that are thermodynamically permissible: namely, that some materials undergo ‘retrograde melting’ when cooled. This peculiar exception to normal melting behavior occurs under unusual circumstances where the entropy of the solid phase is greater than that of its melt at the same temperature and pressure. This can occur in quantum systems, such as solid–liquid He at cryogenic temperatures, and in some classical binary alloy systems at elevated temperatures, where a solid phase will spontaneously melt on cooling. Generally, of course, this is not the case, and the latent heat of fusion,  $\Delta H_f$ , is normally considered to be a positive quantity.

Now, if Eq. (2.1) is substituted into the righthand side of Eq. (2.9), one finds that

$$\Delta H_f = U_\ell - U_s + PV_\ell - PV_s, \quad (2.10)$$

or

$$\Delta H_f = \Delta U_f + P\Delta V_f, \quad (2.11)$$

where  $\Delta V_f \equiv V_\ell - V_s$  is the volume change on melting a mole of material, and  $\Delta U_f \equiv U_\ell - U_s$  is the internal energy change per mole of material melted at the equilibrium melting point.

## 2.2 Comparison of Terms in $\Delta H_f$

Equation (2.11) shows that the enthalpy change for the melting of a pure substance consists of two terms: (1) the internal energy change for the transformation,  $\Delta U_f$ , plus (2) any pressure-volume work,  $P\Delta V_f$ , done by (+), or received from (–), the system’s surroundings, which is taken as standard sea-level atmosphere, where  $P = 0.101$  MPa.

A typical case to be considered here is that of a gram-atomic weight of pure crystalline copper melting gradually at 1,084.6 C (in an equilibrium, or reversible manner) at normal atmospheric pressure. The contributions of the energy terms appearing in Eq. (2.11) for this melting transition are as follows:

1.  $(V_\ell - V_s)/V_s = 0.05$ , and  $V_s = 10.0 \frac{\text{cm}^3}{\text{g}\cdot\text{atom}}$ .
2.  $\Delta V_f = 0.5 \frac{\text{cm}^3}{\text{g}\cdot\text{atom}} = 5.0 \times 10^{-4} \frac{\text{liters}}{\text{g}\cdot\text{atom}}$ .
3.  $P \cdot \Delta V_f = 0.101 \cdot \left( 5.0 \times 10^{-4} \frac{\text{liter}\cdot\text{MPa}}{\text{g}\cdot\text{atom}} \right) \times \left( \frac{1.98}{8.31 \times 10^{-3}} \frac{\text{cal}}{\text{liter}\cdot\text{MPa}} \right)$   
 $= 1.2 \times 10^{-2} \frac{\text{cal}}{\text{g}\cdot\text{atom}}$ .
4.  $\Delta H_f = \Delta U_f + P\Delta V_f = 3 \times 10^3 \frac{\text{cal}}{\text{g}\cdot\text{atom}}$ .

Clearly, the pressure-volume work,  $P\Delta V_f$ , indicated in steps (3) and (4), is negligible compared to the internal energy change  $\Delta U_f$ . This exercise suggests that the enthalpy change for the melting or solidification of a typical metal at atmospheric

pressure is well-approximated by just the change in its internal energy alone. Thus, one may conclude that for most ordinary solidification processes,  $\Delta H_f \approx \Delta U_f$ , which is a result that is accurate under the stated conditions to about 4 ppm! This example also serves to show that the enthalpy (heat content) changes for common solidification and melting processes, i.e., those occurring at or near atmospheric pressure, primarily reflect the large entropy changes occurring during the solid $\leftrightarrow$ melt transformation. The work produced by the volume change acting against the isobaric surroundings is indeed extremely small, and may be safely neglected in most situations.<sup>4</sup>

### 2.3 Co-existence of Solids and Melts

The co-existence of solid and liquid phases under varying thermodynamic conditions presents a classic example of heterophase equilibria, defined by Gibbs as requiring three fundamental conditions:

1. Equality of temperature, or thermal equilibrium, so  $T_s = T_\ell$ .
2. Equality of pressure, or mechanical equilibrium, so that  $P_s = P_\ell$ .
3. Equality of chemical potentials, or chemical equilibrium, so  $\mu_s = \mu_\ell$ .

The internal energies of these conjugate phases are defined as,

$$U_i(S_i, V_i, N_i) = TS_i - PV_i + \mu_i N_i, \quad (i = s, \ell), \quad (2.12)$$

where  $S_i$ ,  $V_i$ , and  $N_i$  are the total entropies, volumes, and molar masses of the phases. The Gibbs potentials for a fixed mass of  $N$  moles, of either solid or melt, are given as,

$$G_i(T, P, N_i) = U_i(S_i, V_i, N_i) - TS_i + PV_i, \quad (i = s, \ell). \quad (2.13)$$

Co-existence of a pure, one-component (unary) crystal and its conjugate melt, expressed through the combined first and second laws, requires unique combinations of temperature and pressure that allow the Gibbs potential per mole, or chemical potential, of the phases to match. Thus, it is required that at thermodynamic equilibrium, Gibbs's heterophase conditions hold, namely

---

<sup>4</sup> The pressure-volume term,  $P\Delta V_f$ , is normally considered as being negligible compared to the internal energy change, excepting when the pressure during solidification exceeds several kilobars. Such conditions do arise in geological solidification and melting of the Earth's mantle rocks, and are even encountered in some important engineering processes carried out at elevated pressure, such as hot isostatic pressing (HIP) of partially molten alloys, squeeze casting, and high-pressure liquid-phase sintering. Generally, however, for melting and freezing under moderate pressures, enthalpy changes alone provide a convenient and reasonably accurate approximation of the internal energy changes.

$$\frac{G_s}{N} = \frac{U_s - TS_s + PV_s}{N} = \frac{G_\ell}{N} = \frac{U_\ell - TS_\ell + PV_\ell}{N}. \quad (2.14)$$

Thermodynamic co-existence of crystal and melt at combinations of temperature and pressure are equivalent to the isothermal, isobaric (reversible) melting of a mole, or gram-atomic weight of crystal, or, similarly, the (reversible) freezing of a mole of melt. These transitions must result in a zero change in the system's Gibbs potential. That is, for reversibly melting a mole of crystal,

$$\frac{G_\ell - G_s}{N} = 0 = \Delta U_f - T \Delta S_f + P \Delta V_f, \quad (2.15)$$

where  $\Delta U_f = (U_\ell - U_s)/N$ ,  $\Delta S_f = (S_\ell - S_s)/N$ , and  $\Delta V_f = (V_\ell - V_s)/N$ , are, respectively, the changes in internal energy, entropy, and volume upon melting one mole of crystal.

Of interest here is determining the condition for solid–liquid phase co-existence where changes in temperature and pressure are allowed, subject to the equality of the chemical potentials, per the Gibbs criterion. The differential form of Eq. (2.15) is

$$0 = d(U_f) - d(T \Delta S_f) + d(P \Delta V_f). \quad (2.16)$$

Substituting the individual total differentials into Eq. (2.16) gives

$$0 = T d(\Delta S_f) - P d(\Delta V_f) - T d(\Delta S_f) - \Delta S_f dT + P d(\Delta V_f) + \Delta V_f dP, \quad (2.17)$$

which after cancellation of terms yields the condition for phase co-existence,

$$0 = -\Delta S_f dT + \Delta V_f dP. \quad (2.18)$$

Equation (2.18) is the Clausius–Clapeyron equation, often written as

$$\left( \frac{dP}{dT} \right)_\mu = \frac{\Delta S_f}{\Delta V_f} = \left( \frac{\Delta H_f}{\Delta V_f} \right) \frac{1}{T_{eq}}. \quad (2.19)$$

The curve along which a pure crystal and its melt maintain equal chemical potentials may be found by integrating Eq. (2.19) from an initial state of co-existence,  $a$ , to another state of co-existence,  $b$ .

$$\int_{P^a}^{P^b} dP = \int_{T_{eq}^a}^{T_{eq}^b} \left( \frac{\Delta H_f}{\Delta V_f} \right) \frac{dT_{eq}}{T_{eq}}, \quad (2.20)$$

which yields the form of the solid–liquid co-existence curve, namely

$$P^b = P^a + \left( \frac{\Delta H_f}{\Delta V_f} \right) \ln \frac{T_{eq}^b}{T_{eq}^a}. \quad (2.21)$$

Equation (2.21) is valid for moderate temperature and pressure changes over which the latent heat of fusion and the volume change on fusion remain reasonably constant. Plots of Eq. (2.21) are shown in Fig. 2.2 for two elements: Pb, an FCC metal, the volume of which expands about 6% on melting, and Si, a diamond-cubic (DC) semiconductor that contracts nearly 10% on melting. The influence of pressure on the melting point of these elements is opposite, because of the sign reversal in their respective volume changes on transforming.

The rather large pressure changes required to shift the melting point of materials just a few K usually makes pressure control impractical for improving the operation of crystal growth processes. High-pressure crystal growth, however, has been employed to elevate the freezing point of certain materials, such as selenium, in order to lower its melt viscosity and augment the rate of crystal growth.

### 2.3.1 Solid-Melt Critical Point

The question has arisen: Could the temperature and pressure be elevated sufficiently to cause a crystal and its co-existing conjugate melt to reach a critical point? Many examples exist, of course, of liquids and vapors having their co-existence curves terminate at critical points. Water and CO<sub>2</sub> are two important examples of liquids exhibiting critical points, and having widespread industrial applications above criticality.

Radial distribution functions for liquid mercury were discussed in Chapter 1, and certainly showed a ‘gas-like’ tendency at high temperatures. But to achieve criticality, two phases must have their molar volume- and entropy-differences *vanish*. These circumstances appear highly unlikely to occur in the case of solids and their melts, as these phases fundamentally differ in their long-range order parameters, whereas liquids and their vapors, below criticality, merely differ in their short-range order parameters. P.W. Bridgman, the Nobel prize winning high-pressure physicist, provides an informed opinion about the above question concerning crystal-melt criticality [5]:

... unless there is some reversal of the trend in the present experimental range at pressures beyond those now attainable, there is no reason to think that the melting [co-existence] curve can end in a critical point.

## 2.4 Thermal Supercooling and Metastability

With reference to the enthalpy-temperature, or  $H$ - $T$ , diagram shown in Fig. 2.3, consider the process of gradually supercooling, or ‘undercooling’, a mole of pure melt phase from the initial state at its equilibrium point,  $T_{eq}$ , to its spontaneous



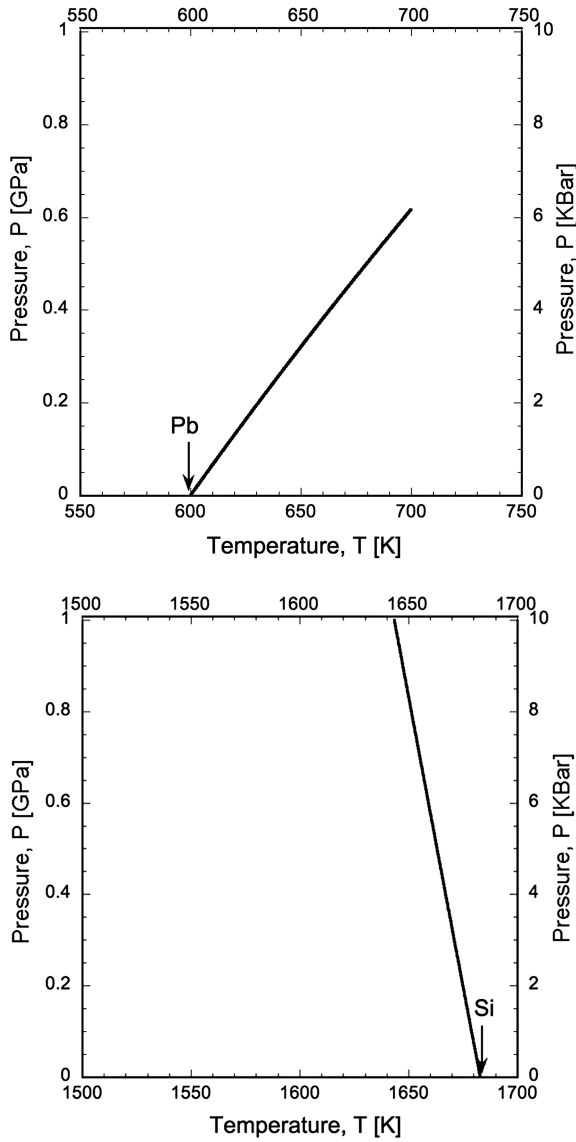


**Fig. 2.2** Co-existence lines on a temperature-pressure phase diagram for crystalline Pb (*upper plot*) and Si (*lower plot*) with their conjugate liquid phases, according to the Clausius–Clapeyron equation, Eq. (2.20). The *vertical arrows* indicate the equilibrium melting points of these elements at ordinary atmospheric pressure. As the pressure increases, the melting point of Pb rises, whereas that of Si decreases. The axes of both plots cover equivalent ranges of temperature and pressure

nucleation temperature,  $T_0$ . The enthalpy change for the liquid cooling from its equilibrium melting point, state  $\ell$ , to its (metastable) supercooled condition, state  $i$ , is  $H_\ell(T_0) - H_\ell(T_{eq})$ . This enthalpy change may be calculated using the standard

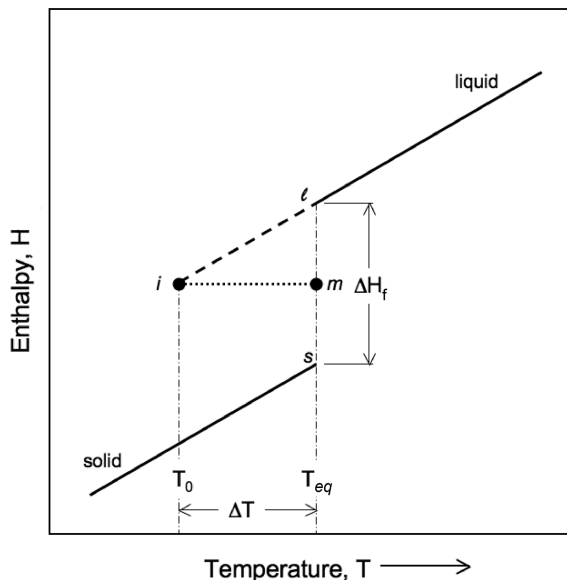


**Fig. 2.3** Enthalpy-temperature diagram for a melt at some fixed pressure, initially in state  $\ell$ , which is then supercooled by an amount  $\Delta T$  to a temperature  $T_0$  below its equilibrium freezing point,  $T_{eq}$ . If the supercooled melt in state  $i$  nucleates and then freezes sufficiently quickly (adiabatically) the system evolves to a ‘mixed’ solid-plus-liquid state,  $m$ , with its average enthalpy,  $H_{s+\ell}$  identical to that of the initially supercooled melt,  $H_\ell(T_0)$ , but comprised of a liquid fraction with molar enthalpy  $H_\ell(T_{eq})$  and a solidified fraction with molar enthalpy  $H_s(T_{eq})$ . The (non-equilibrium) solidification path,  $i \rightarrow m$ , connecting the supercooled and partially solidified states is constrained to be isenthalpic, but only the initial,  $i$ , and end state,  $m$ , have well-defined thermodynamic properties

heat-exchange integral, applying the 1st law of thermodynamics, i.e., conservation of energy,

$$H_\ell(T_0) - H_\ell(T_{eq}) = \int_{T_{eq}}^{T_0} C_p^\ell dT. \quad (2.22)$$

Here, the molar specific heat of the melt phase,  $C_p^\ell \equiv (\partial H_\ell / \partial T)_p$ , represented graphically in Fig. 2.3 as the slope of the liquid-phase existence line, may be considered to be approximately constant for small or moderate amounts of supercooling (typically less than about 100 K). The heat-exchange integral, Eq. (2.22), may be simplified with this approximation and integrated as

$$H_\ell(T_0) = H_\ell(T_{eq}) + C_p^\ell (T_0 - T_{eq}). \quad (2.23)$$

Now, if the supercooled melt, in state  $i$ , is allowed to freeze spontaneously, and the transformation achieves a rate sufficiently fast relative to the time required for long-range heat exchanges with the melt’s surroundings, then an overall *adiabatic*

condition is established between the system and its surroundings. The solidifying system's rapidly (partially) solidified state,  $m$ , is constrained to remain at the same enthalpy level,  $H_m(T_{eq})$ , as the initially supercooled melt, namely,  $H_\ell(T_0) = H_i$ . This type of partial freezing can occur in metals in just a fraction of a second, and is termed adiabatic solidification. Adiabatic solidification results in the production of a well-defined mass fraction,  $X_s$ , of solid from the initially supercooled liquid. The average enthalpy of the resultant two-phase state, (solid plus liquid coexisting at their equilibrium temperature,  $T_{eq}$ ) is equal to the initial enthalpy of the supercooled melt, as no heat has been exchanged with the surroundings. The resultant mass fraction solidified,  $X_s$  may be expressed through the enthalpy conservation condition as

$$H_i = H_m = X_s H_s(T_{eq}) + (1 - X_s) H_\ell(T_{eq}). \quad (2.24)$$

The RHS of Eq. (2.24) is an expression for the average enthalpy of the mixed state,  $m$ . If one equates the RHS of Eqs. (2.23) and (2.24) and solves for the mass fraction frozen adiabatically,  $X_s$ , one obtains the result

$$X_s = \left( \frac{C_p^\ell}{\Delta H_f} \right) \Delta T, \quad (2.25)$$

where in Eq. (2.25) the last term,  $\Delta T = T_{eq} - T_0$ , designates the initial melt supercooling, and the definition for the molar latent heat of fusion is  $\Delta H_f \equiv H_\ell(T_{eq}) - H_s(T_{eq})$ .

### 2.4.1 Characteristic Melt Supercooling

The mass fraction solidifying adiabatically from a supercooled pure melt,  $X_s$ , is referred to in the heat transfer literature as the thermal Stefan number,  $St$ , or dimensionless supercooling. Note  $X_s$  (or, equivalently,  $St$ ) is equal to the dimensionless ratio of the initial supercooling of the melt (in Kelvins) to a property of the system called the 'characteristic' supercooling,

$$\Delta T_{char} \equiv \Delta H_f / C_p^\ell. \quad (2.26)$$

The characteristic supercooling, also expressed in Kelvins, is a thermodynamic property of the melt. Values for the characteristic supercooling of different materials vary widely, however, covering the range of ca. 10–500 K. If a melt were subjected to a supercooling equal to or greater than the melt's characteristic supercooling,  $\Delta H_f / C_p^\ell$ , then  $St \geq 1$ , and the entire melt mass would be capable of solidifying adiabatically, causing  $X_s \rightarrow 1$ . This is the only situation—and one seldom either achieved, or especially desired, in practice—for which *external* heat transfer is not required to complete the solidification process. This extreme condition, and its usually attendant high-speed freezing, have been observed in the laboratory for

small (gram-sized) quantities of many metallic and ceramic materials [6]. By contrast, however, most industrial-scale solidification processes are carried out at levels of supercooling that seldom exceed several Kelvins, and, thus, typically represent only a small fraction of a melt's characteristic supercooling,  $\Delta H_f/C_p^\ell$ . Consequently, in castings, ingots, and welds, as examples of standard industrial solidification processes, the Stefan number for spontaneous freezing is usually small ( $St \ll 1$ ), so little solid is produced promptly and adiabatically following nucleation, and, therefore, external, long-range heat transfer would normally be required to complete the solidification process. The fact that heat must be removed from the crystallizing system and transferred to its environment to allow the major solidification reactions to proceed to completion suggests immediately that heat transfer, unavoidably, is an essential engineering issue in the design of practical solidification and crystal growth processes. Rudiments of solidification heat transfer—both macroscopic and microscopic—will be presented and discussed in subsequent chapters.

Finally, it is worth noting that the subject area of supercooled melts, just touched upon in this section from the energetic standpoint, also extends to a wide range of other interesting materials phenomena. Supercooled (metastable) melts, for example, are relevant to such diverse topics as network (silicate) glass forming systems, phase separating melts, amorphous alloys, crystal growth, atmospheric processes, biological and geological systems, etc. [7, 8].

## 2.5 Free Energy Changes During Freezing and Melting

The ability for any phase transformation to progress spontaneously requires that the system's free energy decreases, or, at a minimum, remains stationary for thermodynamically reversible processes. This statement derives from the 2nd law of thermodynamics [1]. Specifically, for systems held both at constant temperature,  $T$ , and pressure,  $P$ , one chooses the Gibbs potential, or free energy,  $G(T, P, N)$ , as the function testing a solidifying system's stability. The choice of the Gibbs potential is that its functional minima define thermodynamic equilibrium states—both stable and metastable. The Gibbs potential (See Appendix A) is formally defined as the Legendre transform of the system's internal energy,  $U(S, V, N)$ , where temperature,  $T$ , replaces entropy,  $S$ , and pressure,  $P$ , replaces volume,  $V$ , as independent variables [2]. For a gram-atomic, or molar, mass of a unary (single component) system

$$G(T, P, N = 1) \equiv U + PV - TS = H - TS. \quad (2.27)$$

### 2.5.1 Reversible Solidification

The gradual freezing, or melting, of a pure material at its melting temperature,  $T_m$ , and at a fixed pressure,  $P$ , provides a good approximation of a thermodynamically

reversible transformation. For reversible melting or freezing,  $\Delta G = 0$ . Equation (2.27), when applied to the liquid-solid phase change restricted to *reversible* conditions, shows that

$$\Delta H_f = T_m \Delta S_f, \quad (2.28)$$

where the molar entropy of fusion, defined at some pressure,  $P$ , is just the difference in molar entropies between the liquid and crystalline states,

$$\Delta S_f \equiv S_\ell(T_m) - S_s(T_m). \quad (2.29)$$

The molar entropy change,  $\Delta S_f$ , as now defined in Eq. (2.29), is almost always a positive quantity when the solidification-melting reaction proceeds in the direction  $s \rightarrow \ell$ . Thus,  $\Delta S_f$  represents the (normally positive) entropy change associated with the large decrease in long-range atomic order (LRO) as the melting transition proceeds. This sudden decrease in long-range atomic order occurs, as already described in Chapter 1, as a crystal melts to form its conjugate liquid phase at, or close to, its normal thermodynamic melting point. The decrease in LRO increases the system's entropy in direct proportion to the mass of solid melted. The accompanying entropy increase during melting under equilibrium is 'supplied' by *reversible* heat transfers delivered from the system's surroundings. The fact that heat must be added continually from its boundaries so that melting advances over time, again suggests that heat transfer remains a major technical issue in the design of practical melting and solidification processes.

### 2.5.2 Irreversible Solidification

A particularly simple example of irreversible solidification, where  $\Delta G \neq 0$ , is that of the partial adiabatic freezing of a supercooled melt, as shown in the enthalpy diagram, Fig. 2.3. A consequence of irreversibility is that  $\Delta G < 0$  and that  $\Delta S_{tot} > 0$ . The term  $\Delta S_{tot}$  represents the summed entropy changes for the solidifying system plus its surroundings. The 2nd Law of Thermodynamics requires that operating any real (i.e., irreversible) process, where frictional resistance and dissipation are present *at any length scale*, will always increase the total entropy of the universe. Here the word 'universe' may be taken as the crystal-melt system plus its local surroundings, which may be accepting or supplying heat and or work during the irreversible transformation. A formal, and succinct statement of this principle is provided by Clausius's inequality, which states: for any cyclic process or path<sup>5</sup> involving heat exchanges (enthalpy changes) between a system and its surroundings, the closed

---

<sup>5</sup> A 'cyclic' process is a sequence of connected thermodynamic steps, such as heat transfer, work exchanges, and transformations, all of which eventually returns the system and its surroundings to their initial states.

line integral of the irreversible heat exchanged, divided by the absolute temperature, along any segment of the cycle must be less than the line integral taken along the same path for reversible heat exchange. Thus,

$$\oint \frac{\hat{d}Q}{T} \leq \oint \frac{\hat{d}Q_{rev}}{T}. \quad (2.30)$$

For segments of the cyclic pathway that are reversible, the RHS of Eq. (2.30) equals the change in the classical entropy for the system, or minus the same entropy change for the surroundings with which the reversible heat exchanges occur.

$$\Delta S_{sys} = -\Delta S_{surr} = \oint \frac{\hat{d}Q_{rev}}{T}. \quad (2.31)$$

The path integral of reversible heat exchanges thus encompasses a series of state function changes. For a cyclic path, the starting point equals the end point, and this line integral for reversible processes vanishes. If, however, irreversible steps are anywhere involved, such as in the rapid solidification of a supercooled melt, then the value of the integral on the LHS of Eq. (2.30) will always be *less* than that of the one traversing the reversible cycle.

Now, as mentioned, entropy,  $S$ , like enthalpy,  $H$ , is a thermodynamic state function. So, even if a cyclic thermodynamic path involves some irreversibility, it follows that for *any* segment of the cycle connecting two states, say the initially supercooled melt,  $i$ , and the partially frozen mixture,  $m$ , shown in Fig. 2.3, the entropy change between those states must be identical. This remains true whether or not these state changes are accessed via either reversible or irreversible processes. Thus, *irrespective of path reversibility*,

$$\Delta S_{irrev}[i \rightarrow m] = \Delta S_{rev}[i \rightarrow m]. \quad (2.32)$$

If, however, the process connecting states  $i$  and  $m$  is a real one, and dissipation, or friction, is present, one expects some additional entropy to be produced within the system that does not involve any heat exchange with the surroundings. Indeed, the spontaneous fast freezing of a metastable, supercooled melt involves complex internal mesoscopic heat transfer (occurring on a scale of millimeters or micrometers) under extremely steep thermal gradients, and the process entails rapid molecular attachment and growth of the interphase interfaces. Interface growth and propagation requires irreversible atomic motions (occurring over microscopic dimensions of fractions of a nanometer). The additional entropy production,  $\Delta S_{prod}$ , incurred by free energy dissipation is indistinguishable from, and added to, any entropy changes directly caused by heat exchanges with the surroundings. So for any irreversible segment it follows that,

$$\Delta S_{irrev} = \int \frac{\hat{d}Q}{T} + \Delta S_{prod}. \quad (2.33)$$

In view of Eqs. (2.32) and (2.31), one sees that the Clausius inequality, Eq. (2.30), must be obeyed, as  $\Delta S_{prod} > 0$ , and the integral of the heat exchange divided by the absolute temperature for an irreversible cycle will always be smaller than that for a reversible cycle. In Section 2.7 we will develop the details of such a comparison with an irreversible solidification process.

## 2.6 Principal Types of Binary Alloy Solidification

Many of the theoretical models, examples, and experiments, discussed throughout this book are directed at so-called ‘engineering’ materials. These are often, but not exclusively, metals and alloys that are melted, cast, soldered and welded in the course of their production, fabrication, and application. The microstructures, solidification responses, and properties of numerous commercial casting alloys have been studied intensively, and reported in detailed microstructure atlases [9], usually organized broadly under categories based on the main elemental component (e.g., copper alloys, aluminum alloys, cast irons and steels). These microstructure atlases are invaluable for their practical guidance on alloy selection and subsequent processing, but the underlying scientific principles explaining the origin and formation of their cast microstructures are seldom included. In addition to ordinary casting alloys, solidification principles are also applicable to the production and control of sophisticated high-temperature alloy castings, composed of large, shaped, super-alloy single crystals for use in critical applications, such as jet aircraft engines and large land-based turbo-generators. The fundamental approaches to be described here also apply to other important classes of modern materials [10], such as the preparation of semiconductors [11, 12], superconductors [13], and opto-electronic materials [14]. Nevertheless, some of the best confirmation of the theories and explanations to be presented in later chapters are for binary alloys that often form the starting point for the development of practical engineering materials, the economic importance of which to modern society is nothing short of extraordinary.

The following discussion is based upon a generic binary phase diagram [15] that captures the major phase relationships applicable to some of the typical alloys to be treated in detail in later chapters.

1. (*A* & *B*) are the pure components: The components of a binary alloy locate the ends of the diagram (See Fig. 2.4.), and typically solidify from their respective supercooled melts as pure *A*- or *B*-dendritic (branched) crystals, or, as a slowly grown, smooth solidification front, leading to nearly featureless monocrystals. Pure materials provide limited applications, aside perhaps from some major importance as metallic electrical conductors and semiconductors. Pure materials tend to be too weak mechanically for most other engineering applications. They do afford, however, the simplest examples for studying the solidification process.
2. (*SS*) solid solution alloys: Such dilute alloys typically solidify as  $\alpha$ - or  $\beta$ -phase solid-solution ‘primary’ dendrites, along with small amounts of non-equilibrium phases that eventually appear within the cast microstructure. Binary solid

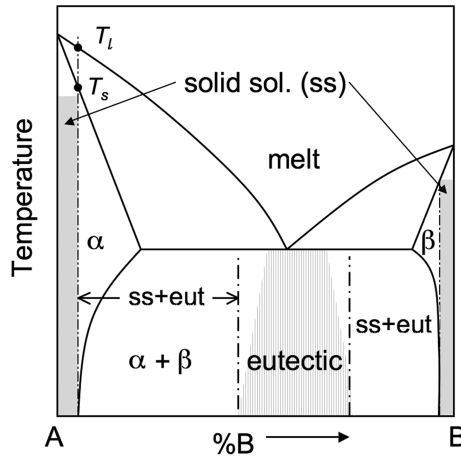


**Fig. 2.4** Binary phase diagram, displaying some typical compositional zones that exhibit distinctive solidification behaviors. The curves  $T_l$  and  $T_s$  indicate the liquidus and solidus boundaries, which track the temperatures where equilibrium solidification starts,  $T_l$ , and completes,  $T_s$ , at a given composition, %B, and temperature. The shaded ‘terminal’ regions, located near the pure components A and B, are labeled ‘ss’, which denotes the limited composition zones for obtaining single-phase microstructures of either of the two solid-solution phases,  $\alpha$  or  $\beta$ . The gray area, labeled ‘eutectic’, located around the mid-composition range, indicates where the eutectic microstructural constituent dominates during freezing. The two regions, ‘ss+eut’, suggest compositions over which the microstructure consists of primary phase and some eutectic microconstituent. Adapted from [15]

solutions are a step closer to practical casting alloys, which usually contain at least three, or more, controlled elemental components. More complex alloys cast for specialty purposes, such as tool steels, stainless steels, aero-structural alloys, or superalloys for high-temperature applications may contain over a dozen controlled components!

3. (*SS + Eu*) solid solution primary phase + eutectic: More solute-rich alloys initially solidify as either  $\alpha$ - or  $\beta$ -dendrites, depending on composition, accompanied by a significant amount of  $\alpha/\beta$  eutectic micro-constituent, appearing later in the overall freezing process. The eutectic constituent is often distributed throughout the interdendritic spaces of each grain in a casting. This is probably the most common situation encountered in practical casting alloys.
4. (*Eu*) Eutectic (polyphase): Binary eutectics solidify by an isothermal  $\alpha/\beta$  eutectic reaction. Many eutectics are characterized by relatively short-range diffusion paths among  $\alpha$ ,  $\beta$ , and the eutectic melt from which they crystallize in close proximity. Eutectic binary alloys form the basis for common solders and brazing alloys, as well as cast irons and type metal. Polyphase solidification, as occurs in eutectic alloys, involves complex interfacial and diffusion processes among the three phases, and will be discussed in more detail in Chapter 16.

The reader should note at this point that the major distinction among solid-solution dendritic alloys and eutectics is primarily the scale at which the



solidification structure forms. Eutectics tend to develop fine-scale microstructures (ca. 1–10  $\mu\text{m}$ ), whereas dendritic structures exhibit relatively coarse morphologies (ca. 10–100  $\mu\text{m}$ ). Every alloy type yields a range of cast structures that depends sensitively on the alloy's chemical composition, initial superheating of the melt, solidification geometry and mold-wall characteristics, supercooling and cooling rate, plus ‘modifiers’ that may be added as grain refiners or to control gas porosity.

## 2.7 Illustrative Examples

One gram-atom of pure aluminum is melted and held at its equilibrium temperature,  $T_{eq}$ , at atmospheric pressure,  $P$ . This melt, held in a well-insulated inert crucible, is then supercooled to a lower temperature,  $T_0$ , nucleated, and then (partially) solidified adiabatically. The remainder of the melt, after partial adiabatic freezing, is subsequently totally re-solidified at its equilibrium temperature,  $T_{eq}$ , by slowly withdrawing heat from the container. The following thermo-chemical data apply:

- Gram-atomic mass Al = 26.98 g
- $T_{eq} = 933.2\text{ K}$
- $\Delta T = T_{eq} - T_0 = 60\text{ K}$
- $\Delta H_f = 10.47 \frac{\text{kJ}}{\text{g-atom}}$
- $\Delta T_{char} = \Delta H_f / C_p^\ell = 375.5\text{ K}$
- $C_p^\ell = 28.74 \frac{\text{J}}{\text{g-atom}\cdot\text{K}}$
- $S_s(T_{eq}) = 59.18 \frac{\text{J}}{\text{g-atom}\cdot\text{K}}$
- $S_\ell(T_{eq}) = 71.13 \frac{\text{J}}{\text{g-atom}\cdot\text{K}}$

1. *Once nucleated, how many grams of crystalline Al freeze adiabatically from the initially supercooled melt?*

When supercooled by 60 K, molten Al can nucleate and spontaneously freeze, forming a mass fraction of solid phase,  $X_s$ . Spontaneous solidification of Al at this large supercooling is rapid, so partial freezing occurs under virtually adiabatic conditions. The latent heat released is trapped within the insulated system, quickly raising the temperature of the solid–liquid mixture to its equilibrium melting point,  $T_{eq}$ , at which time further solidification ceases. The mass fraction of Al crystals,  $X_s$ , solidifying to the end-point of adiabatic freezing may be found using energy conservation, by applying the ‘lever rule’ to the metastable extension of the enthalpy-temperature, H-T, phase diagram. See again, Fig. 2.3 to follow these geometric constructions:

$$X_s = \frac{\ell m}{\ell_s}, \quad (2.34)$$

where  $\ell m/im = C_p^\ell$ ,  $im = T_{eq} - T_0$ , and  $\ell s = \Delta H_f$ . Substituting all these quantities into the RHS of Eq. (2.34) yields the mass fraction of solid Al

$$X_s = \frac{T_{eq} - T_0}{\Delta H_f / C_p^\ell} = \frac{\Delta T}{\Delta T_{char}} = 0.16. \quad (2.35)$$

The mass of Al,  $M_s$ , solidified adiabatically is therefore  $0.16 \times 26.98 \text{ g} = M_s = 4.3 \text{ g}$ . This leaves a mass of untransformed liquid Al,  $M_\ell = 22.68 \text{ g}$ , with the system adiabatically self-heated back to its equilibrium temperature,  $T_{eq} = 933.2 \text{ K}$ . The crystals and melt produced by partial adiabatic freezing are usually found in the form of a fine mixture, or slurry of dendrites, called a ‘mush’. The scale, morphological characteristics, and kinetic behavior of rapidly formed solidification microstructures comprise interesting important topics, and are dealt with in Chapters 13 and 17.

2. *Determine the entropy change for the partial adiabatic freezing described in (1).* First, with reference to Fig. 2.5, the *reversible* entropy change per g-atom Al solidified slowly at its equilibrium point,  $T_{eq}$ , is  $-\Delta S_f = S_s(T_{eq}) - S_\ell(T_{eq}) = -11.95 \text{ [J/g-atom}\cdot\text{K]}$ . Next, the entropy per g-atom of the initially supercooled melt,  $S_\ell(T_{eq} - 60 \text{ K})$ , may be found by calculating the Clausius heat exchange integral, Eq.(2.31), for the liquid phase cooled slowly and reversibly from its equilibrium temperature,  $T_{eq}$ , into its supercooled state at  $T_{eq} - 60 \text{ K}$ . One obtains

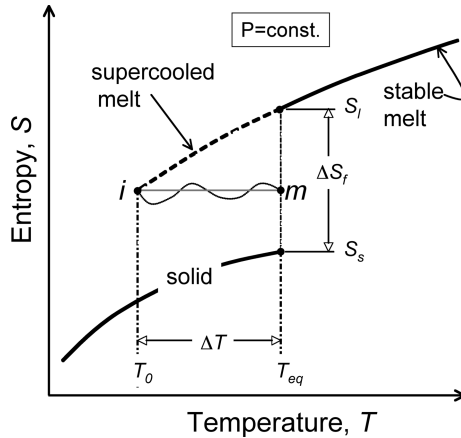


**Fig. 2.5** Entropy-temperature,  $S$ - $T$ , diagram for a pure melt. The entropies for the stable crystalline solid and liquid phases are shown as *solid curves*. The entropy for the metastable supercooled melt is the *dashed curve* extending below  $T_{eq}$  of the stable melt. The wiggly curve connecting the entropy for the initially supercooled melt, and the resultant mixed-state of solid plus melt at  $T_{eq}$  suggests some unknown non-equilibrium pathway for rapid adiabatic solidification. Irreversible pathways cannot be displayed on the  $S$ - $T$  equilibrium phase diagram

$$S_\ell(T_{eq} - 60 \text{ K}) = S_\ell(T_{eq}) + \int_{T_{eq}}^{T_{eq} - 60 \text{ K}} C_p^\ell \frac{dT}{T}. \quad (2.36)$$

Substituting values into Eq.(2.36) from the list of thermochemical data for Al yields the entropy per mole of molten Al cooled 60 K below its equilibrium temperature,

$$\begin{aligned} S_\ell(T_{eq} - 60 \text{ K}) &= 71.13 + 28.74 \times \left( \ln \frac{933.2 \text{ K} - 60 \text{ K}}{933.2 \text{ K}} \right) \\ &= 69.22 \left[ \frac{\text{J}}{\text{g} - \text{atom} \cdot \text{K}} \right], \end{aligned}$$

As might be expected, supercooled (metastable) molten Al is found to have a lower entropy per unit mass than does (stable) molten Al at its melting point.

The entropy of the mixed state (crystal plus melt) formed immediately after partial adiabatic freezing may be determined by using the rule of mixtures, recognizing that the mass fractions of solid and melt are also equivalent to their atom fractions in the partially solidified mixture, and that entropy—a thermodynamic state function—is independent of the path taken between the initial (supercooled) and final (partially solidified) states. Thus,

$$S_{mixed} = S_s(T_{eq}) \cdot X_s + S_\ell(T_{eq}) \cdot X_\ell, \quad (2.37)$$

and so

$$S_{mixed} = (59.18)(0.16) + (71.13)(0.84) = 69.22 \left[ \frac{\text{J}}{\text{g} - \text{atom} \cdot \text{K}} \right],$$

Comparison of Eq. (2.36) and Eq. (2.37) shows that the molar entropy change caused by adiabatically freezing the supercooled melt to a mixed state containing about 16% crystalline Al at  $T_{eq}$  is exactly zero. As heat flow during *adiabatic* freezing is precluded either to or from the system's external environment, one may conclude that the environment itself does not experience any entropy change during the partial freezing process.

Any entropy production attending the irreversible solidification cycle will therefore depend on certain (unknown) kinetic details of the non-equilibrium (irreversible) phenomena that accompanied the rapid solidification process. Non-equilibrium solidification and crystal growth phenomena will be discussed in Chapter 17.

The cyclic value of Clausius's heat exchange integral may be evaluated for adiabatic solidification by starting with the melt at its equilibrium temperature,  $T_{eq}$ , and then (1) reversibly cooling it to its initial metastable state at a supercooling  $\Delta T = T_{eq} - T_0$ ; (2) allowing adiabatic solidification to occur ( $\Delta Q = 0$ ); (3) then reversibly remelting the fraction of solid,  $X_s$ , and, thereby, returning the system to its starting condition at  $T_{eq}$ .

$$\oint \frac{\hat{d}Q}{T} = \int_{T_{eq}}^{T_0} \frac{C_p^\ell dT}{T} + 0 + X_s \frac{\Delta H_f}{T_{eq}}. \quad (2.38)$$

Evaluating the integral on the RHS of Eq. (2.38), substituting Eq. (2.35) for the coefficient  $X_s$ , and then canceling terms yields

$$\oint \frac{\hat{d}Q}{T} = C_p^\ell \ln \left( \frac{T_0}{T_{eq}} \right) + C_p^\ell - C_p^\ell \frac{T_0}{T_{eq}}. \quad (2.39)$$

Division of both sides of Eq. (2.39) by the common factor,  $C_p^\ell$ , provides a dimensionless form of the cyclic heat integral, namely,

$$\mathcal{I}(\rho) = \ln \rho + 1 - \rho, \quad (2.40)$$

where  $\mathcal{I}(\rho)$  is the dimensionless heat exchange integral, and  $\rho \equiv T_0/T_{eq}$  is the ratio of the nucleation temperature,  $T_0$ , to the equilibrium temperature. A plot of Eq. (2.40) is shown in Fig. 2.6.

3. Find the additional entropy change for isothermally (reversibly) freezing the remaining molten Al at its melting temperature.

The remaining 22.7 g of molten Al can be solidified by gradually transferring the required amount of latent heat to the system's surrounding at the equilibrium

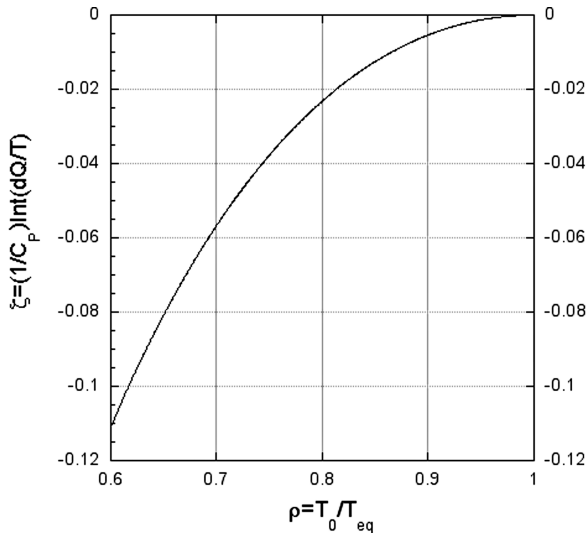


**Fig. 2.6** Plot of Eq. (2.40), showing the cyclic heat exchange integral for irreversible adiabatic solidification. Note that the function,  $\zeta$ , is always negative, in agreement with Clausius's inequality [1], Eq.(2.30), confirming that the cyclic heat exchanged between a solidifying system and its surroundings is *always* less than that for a reversible cycle, where Clausius's integral vanishes

temperature,  $T_{eq}$ . Slow, isothermal solidification under negligible thermal gradients approximates reversible heat transfer from the surroundings.

Thus, the Clausius inequality may also be stated as,

$$\Delta S \geq \oint \frac{\hat{d}Q_{irr}}{T}. \quad (2.41)$$

The reversible entropy change for the remaining melt to be solidified at its equilibrium temperature is

$$\Delta S_{rev} = \frac{(59.18 - 71.13) \left[ \frac{\text{J}}{\text{g-atom}\cdot\text{K}} \right] \times 22.7 [\text{g}]}{26.98 \left[ \frac{\text{g}}{\text{g-atom}} \right]} = -10.05 \left[ \text{J} \cdot \text{K}^{-1} \right], \quad (2.42)$$

The system's surroundings that receive the latent heat released from solidifying the remaining melt would, of course, increase its entropy by the same, or greater amount, thus, satisfying Clausius's inequality, Eq. (2.41). Were this last portion of the solidification cycle (slow freezing) truly reversible, its added entropy change for the system plus its surroundings would be zero.

4. *What is the enthalpy change for partial adiabatic freezing?*

The enthalpy, a thermodynamic function of state, can also be used to characterize adiabatic freezing. The molar enthalpy change may be found simply as,  $\Delta H_{tot} = H_{final} - H_{initial}$ . The final system enthalpy,  $H_{final}$ , may be found again using the rule of mixtures, namely

$$H_{final} = H_{\ell}(T_m)(0.84) + H_s(T_m)(0.16), \quad (2.43)$$

so that

$$H_{final} = H_{\ell}(T_m)(0.84) + (H_{\ell}(T_m) - \Delta H_f)(0.16), \quad (2.44)$$

and

$$H_{final} = H_{\ell}(T_m) - 1.68 \left[ \frac{\text{kJ}}{\text{g-atom}} \right]. \quad (2.45)$$

The initial enthalpy of the supercooled melt can be calculated using the heat integral, remembering that  $C_p^{\ell}$  is approximately constant over moderate temperature changes.

$$H_{initial} = H_{\ell}(T_m) + \int_{T_m}^{T_m-60} C_p^{\ell} dT \approx H_{\ell}(T_m) - 28.74 \left[ \frac{\text{J}}{\text{g-atom}} \right] \times 60. \quad (2.46)$$

so

$$H_{initial} = H_{\ell}(T_m) - 1.72 \left[ \frac{\text{kJ}}{\text{g} - \text{atom}} \right]. \quad (2.47)$$

Subtracting the results found in Eq. (2.47) from that found in Eq. (2.45) shows that the total change in enthalpy, within the precision of these calculations, is  $\Delta H_{tot} = H_{final} - H_{initial} \approx 0$ . A zero net change in the total enthalpy is the result expected for any ‘isenthalpic’ process, such as adiabatic solidification. (See again Fig. 2.3.) In essence, the partial solidification process merely ‘rearranged’ the internal distribution of the system’s enthalpy (heat content), but does not alter its total value. We shall discover later that cast alloy microstructures evolve through the spatial redistribution of both enthalpy and chemical components. An advantage of using the enthalpy function,  $H$ , to follow energy changes during solidification, rather than using the classical entropy,  $S$ , is that the influence of the (constant pressure) environment is automatically accounted in the calculations.

5. *Estimate the Gibbs free energy change for the spontaneous partial solidification of the supercooled melt.*

The initial state of the system, prior to its partial freezing, is metastable melt phase supercooled 60 K. See the Gibbs potential versus temperature plot, Fig. 2.7. The Gibbs free energy per mole of the solid and melt are equal at the mixture’s final equilibrium temperature,  $T_{eq}$ , and pressure,  $P$ . The Gibbs free energy change per mole solidified may be found as the difference between the

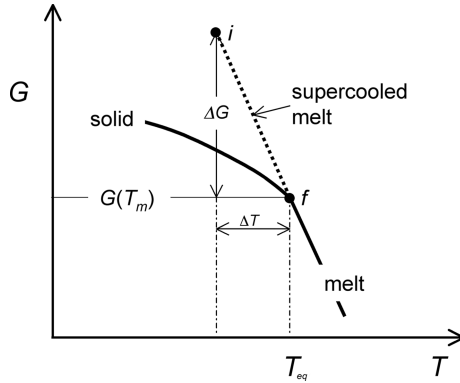


**Fig. 2.7** Gibbs free energy versus temperature. The stable phases are shown as *solid* curves that intersect at the equilibrium melting temperature,  $T_{eq}$ . The Gibbs energy for the metastable melt, which is supercooled an amount  $\Delta T$ , is represented as the *dotted* extension of the stable melt curve below  $T_{eq}$ . The initial supercooled melt has its free energy at point  $i$ , and the final state of the partially solidified two-phase mixture is shown at point  $f$ . The total change in Gibbs free energy for spontaneous partial freezing is shown as the vertical drop,  $\Delta G$ , from states  $i \rightarrow f$ . The non-equilibrium path actually connecting states  $i$  and  $f$  cannot be represented on this diagram.

free energy in the final (partially solidified) state,  $f$ , and the initial (fully molten) supercooled state,  $i$ .

$$\Delta G = G_{final} - G_{initial} = G(T_{eq}) - G_{\ell}(T_{eq} - \Delta T). \quad (2.48)$$

The change in free energy for supercooling the melt from state  $f \rightarrow i$  is given as

$$G(T_{eq}) - G_{\ell}(T_{eq} - \Delta T) = \int_{T_{eq}-\Delta T}^{T_{eq}} S_{\ell} dT \approx S_{\ell}(T_{eq}) \cdot \Delta T, \quad (2.49)$$

where the approximation is employed of considering the entropy of the melt to remain constant. Using the thermochemical data provided, the Gibbs free energy change per mole of supercooled melt that spontaneously solidifies (states  $i \rightarrow f$ ) is given by  $-S_{\ell}(T_{eq}) \cdot \Delta T$ , and thus,

$$\Delta G = -71.13 \left[ \frac{\text{J}}{\text{g} - \text{atom} \cdot \text{K}} \right] \times 60 \text{ K} = -4.27 \left[ \frac{\text{kJ}}{\text{g} - \text{atom}} \right], \quad (2.50)$$

which, indeed, represents a relatively large release of free energy. Although the irreversible path connecting the initial supercooled melt, point  $i$ , and the system's final mixed-phase state, point  $f$ , cannot be traced directly on the free energy diagram, the net free energy change between these states is easily found. A negative value of the Gibbs energy change is *always* required for spontaneous (thermodynamically permissible) physical processes such as adiabatic solidification.

6. Show that for (reversible) isothermal freezing of the rest of the melt, controlled through extremely slow external heat transport, the Gibbs free energy change  $\Delta G = 0$ .

The Gibbs function was defined earlier in Eq. (2.7) as  $G = H - TS$ . For an isothermal, isobaric process, such as the slow solidification of a pure material at its equilibrium temperature, the change per gram-atom of the Gibbs potential is

$$\Delta G = \Delta H_f - T \Delta S_f. \quad (2.51)$$

Substituting Eq. (2.8) for the enthalpy of fusion,  $\Delta H_f$ , in Eq. (2.51), which is a valid relationship for isobaric, isothermal, reversible phase changes, proves that  $\Delta G = 0$ . This result for slow equilibrium (reversible) solidification contrasts with our earlier finding in exercise (5) for spontaneous solidification, which always results in a negative free energy change.

The key difference demonstrated here between *reversible* and *irreversible* solidification processes is that in the latter case at least some free energy would be consumed by unavoidable kinetic processes attending the rapid solidification reaction. Non-equilibrium processes in rapid solidification are discussed in later chapters, and include transport of latent heat, diffusion of solutes (in the case of alloys), viscous flows in the melt, solid–liquid interface growth and motion, and, finally, formation of non-equilibrium crystalline defects generated within

the solid phase as a crystal grows rapidly. These defects include trapped excess lattice vacancies and solutes, reduced crystallographic order, dislocation networks, mosaic structures, and grain boundaries; any or all may result when a supercooled melt nucleates spontaneously and crystals grow rapidly.

## 2.8 Summary

This chapter introduces the notions of heat and work associated with solid–liquid transformations at constant pressure. The first law of thermodynamics is used to discuss the magnitudes of these contributions to the enthalpy, or heat content function, showing that conventional melting and freezing processes carried out near ambient pressures have negligible pressure-volume terms compared to their internal energy changes as regarding the magnitude of the latent heat of transformation. The internal energy change itself reflects primarily the entropy change associated with the loss, or gain, of long-range order upon melting, or freezing, respectively. Major exceptions to this conclusion occur in cases of melting and freezing at kilobar pressure levels, which are indeed common in geological solidification of mantle rocks, and in some industrial high-pressure liquid metal sintering processes.

The coexistence conditions for crystals and their conjugate melt phases are developed using the so-called combined first and second laws of thermodynamics. The Gibbs criterion for heterophase equilibrium is introduced, requiring that mechanical, thermal, and chemical equilibria all occur simultaneously. The Clausius–Clapeyron equation is then derived to specify the allowed combinations of temperature and pressure that equate the chemical potentials of a crystal and its melt, and thus permitting solid–liquid co-existence to occur.

Next, the important concepts of phase metastability and thermal supercooling are introduced, using the simple example of a pure melt, sub-cooled below its thermodynamic freezing point, and then allowed to freeze adiabatically. These concepts occur multiple times in various contexts as subsequent chapters cover kinetic topics where supercooling and metastability arise as factors. Associated with these concepts are the foundational ideas of reversible and irreversible processes. The Clausius inequality is used to explain the precise thermodynamic criterion for distinguishing between reversible and irreversible processes. To make those abstractions more concrete, detailed calculations are used as examples of the entropy production and free energy dissipation that are encountered during irreversible freezing.

Finally, binary alloy solidification is introduced by discussing a few generic types of solidification alloys: (1) unary, or one-component freezing; (2) binary solid-solution alloys; (3) solid-solution plus eutectic microconstituents; and (4) polyphase solidification, such as eutectics and peritectics. Some illustrative thermochemical calculations are also provided covering the simpler case of freezing pure aluminum both adiabatically and isothermally, where the cyclic heat exchange is explored as a measure of irreversibility, and Gibbs potential changes are calculated to distinguish reversible and irreversible solidification clearly.



## References

1. W.J. Moore, *Physical Chemistry*, 2nd Ed., Prentice-Hall, Inc., Englewood Cliffs, NJ, 1955.
2. H.B. Callen, *Thermodynamics and an Introduction to Thermostatistics*, 2nd Ed., Wiley, New York, NY, 1985.
3. R.T. DeHoff, *Thermodynamics in Materials Science*, Chap. 3, McGraw-Hill, Inc. New York, NY, 1993.
4. M. Stier and M. Rettenmayr, *J. Cryst. Growth*, **311** (2008) 137.
5. P.W. Bridgman, *Physics of High Pressure*, Bell, London, 1949.
6. 'Undercooled metallic melts: properties, solidification and metastable phases', *Proceedings of the NATO Advanced Research Workshop*, D.M. Herlach, I. Egry, P. Baeri and F. Spaepen, Eds., II Ciocco, Italy, 1993.
7. J.T. Fourkas et al., *Supercooled Liquids*, ACS Symposium Series 676, American Chemical Society, Washington, DC, 1997.
8. *Schmelze, Erstarrung und Grenzflächen*, I. Egry, P.R. Sahm and T. Volkmann, Eds., Vieweg Verlag, Braunschweig, 1999.
9. L. Backerud, C. Guocai and J. Tamminen, *Solidification Characteristics of Aluminium Alloys*, **2**, American Foundry Society, Des Plaines, IL, 1990.
10. *Solidification Science and Processing*, I. Ohnaka and D.M. Stefanescu Eds., TMS, Warrendale, PA, 1996.
11. *Crystal Growth*, C.H.L. Goodman, Ed., **1**, Plenum Press, New York, NY, 1978.
12. *Crystal Growth*, C.H.L. Goodman, Ed., **2**, Plenum Press, New York, NY, 1978.
13. Y. Yamada, *J. Mater. Res.*, **10** (1995) 1601.
14. N.B. Singh et al., *J. Cryst. Growth*, **250** (2003) 107.
15. W. Kurz and D.J. Fisher, *Fundamentals of Solidification*, Chap. 1, 3rd Ed., Trans Tech Publications, Aedermannsdorf, 1989.

Principles of Solidification

An Introduction to Modern Casting and Crystal Growth  
Concepts

Glicksman, M.E.

2011, XVIII, 520 p., Hardcover

ISBN: 978-1-4419-7343-6